

# Sampling Medium Side Resistance to Uptake of Semivolatile Organic Compounds in Passive Air Samplers

Xianming Zhang,<sup>†</sup> Masahiro Tsurukawa,<sup>‡,§</sup> Takeshi Nakano,<sup>‡,§,||</sup> Ying D. Lei,<sup>†</sup> and Frank Wania<sup>\*,†</sup>

<sup>†</sup>Department of Chemistry and Department of Physical and Environmental Sciences, University of Toronto Scarborough, Toronto, Ontario M1C 1A4, Canada

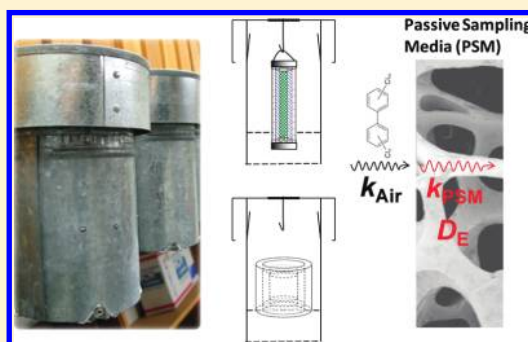
<sup>‡</sup>Hyogo Prefectural Institute of Environmental Sciences, 3-1-27, Yukihira-cho, Suma-ku, Kobe 654-0037, Japan

<sup>§</sup>Graduate School of Engineering, Osaka University, 2-1, Yamadaoka, Suita 565-0871, Japan

<sup>||</sup>Graduate School of Maritime Science, Kobe University, 5-1-1, Fukaeminamimachi, Higashinada-ku, Kobe 658-0022, Japan

**S** Supporting Information

**ABSTRACT:** Current theory of the uptake of semivolatile organic compounds in passive air samplers (PAS) assumes uniform chemical distribution and no kinetic resistance within the passive sampling media (PSM) such as polystyrene-divinylbenzene resin (XAD) and polyurethane foam (PUF). However, these assumptions have not been tested experimentally and are challenged by some recently reported observations. To test the assumptions, we performed kinetic uptake experiments indoors using cylindrical PSM that had been concentrically segmented into three layers. Both XAD and PUF were positioned in the same type of sampler housing to eliminate the variation caused by the different housing designs, which enabled us to quantify differences in uptake caused by the properties of the PSM. Duplicated XAD (PUF) samples were retrieved after being deployed for 0, 1 (0.5), 2 (1), 4 (2), 8 (4), 12 (8), and 24 (12) weeks. Upon retrieval, the PSM layers were separated and analyzed individually for PCBs. Passive sampling rates ( $R$ ) were lower for heavier PCB homologues. Within a homologue group,  $R$  for XAD was higher than that for PUF, from which we infer that the design of the “cylindrical can” housing typically used for XAD PAS lowers the  $R$  compared to the “double bowl” shelter commonly used for PUF-disk PAS. Outer layers of the PSM sequestered much higher levels of PCBs than inner layers, indicative of a kinetic resistance to chemical transfer within the PSM. The effective diffusivities for chemical transfer within PSM were derived and were found negatively correlated with the partition coefficients between the PSM and air. Based on the results, we conclude that the PSM-side kinetic resistance should be considered when investigating factors influencing  $R$  and when deriving  $R$  based on the loss of depuration compounds.



## INTRODUCTION

Dynamic-uptake based passive air samplers (PAS) such as those based on polystyrene divinylbenzene (XAD)<sup>1</sup> and polyurethane foam (PUF)<sup>2</sup> are increasingly used to study persistent semivolatile organic compounds (SVOCs) in the atmosphere. Such PAS are capable of time-integrated sampling with relatively low cost and simple operation, which is independent from power supply and free of noise.<sup>1–3</sup> Because of these advantages over the traditional high-volume air sampler, PAS are widely applied to understand spatial and long-term temporal trends, identify sources, and assess human exposure to SVOCs in various types of environments.<sup>4–6</sup>

The mechanism of uptake in PAS is based on the molecular diffusion from air to passive sampling medium (PSM). Conceptually, the process of SVOC uptake in PAS has been described using the two-film diffusion model,<sup>2,7</sup> which was originally proposed to describe mass transfer across gas–liquid interfaces.<sup>7</sup> According to the two-film model, “in the main body of either liquid and gas, ...the concentration of solute in the fluid is essentially uniform at all

points”.<sup>7</sup> As indicated by the current PAS “theory”,<sup>2,3</sup> the kinetic resistance within the PSM is inversely related to a chemical’s PSM/air partition coefficient and thus negligible for SVOCs due to their large PSM/air partition coefficients. Therefore, the resistance posed by the air boundary layer is regarded as controlling the rate of SVOC uptake in PAS. During the initial uptake stage (operationally defined as the linear uptake range), chemical concentrations on the PSM are so low that surface evaporation is negligible. As such, chemical uptake in PAS can be quantified with a simple linear equation involving a sampling rate ( $R$ , m<sup>3</sup>/d) that only depends on the surface area of the PSM, the chemical’s molecular diffusivity in air ( $D_A$ ), and the boundary layer thickness.<sup>3</sup> Because the boundary layer thickness is difficult to quantify directly, in practice,  $R$  is usually determined by

**Received:** June 30, 2011

**Accepted:** November 2, 2011

**Revised:** October 25, 2011

**Published:** November 02, 2011

calibrations against air concentrations determined using active samplers.

A number of PAS calibration studies have determined  $R$  for both XAD-PAS and PUF-PAS under different environmental conditions.<sup>1,8–12</sup> Based on these studies, XAD-PAS have a higher sampling capacity or longer linear uptake range than PUF-PAS.<sup>13</sup> The high capacity makes XAD-PAS superior for integrated sampling over long time periods, especially for relatively more volatile compounds such as the fluorotelomer alcohols.<sup>14</sup> However, XAD-PAS generally have a 2- to 5-fold lower  $R$  than PUF-PAS. So far, it is unclear whether the different  $R$  is caused by differences in the properties of XAD and PUF or by differences between the housing configurations typically employed with the two PAS.

$R$  for both of the PAS varies among different chemicals or at different temperatures.<sup>9–11,15</sup> Such variations are larger than can be explained by the dependence of  $D_A$  on chemical properties or temperature (Fuller–Schettler–Giddings equation),<sup>16</sup> indicating some other influential factors may exist. For the PUF-PAS, some studies observed higher  $R$  for chemicals with lower volatility,<sup>11,17</sup> an observation attributed to the binding of such chemicals to particles, which are trapped by the PUF. Conflicting results showing lower  $R$  for particle-bound chemicals have also been found.<sup>15</sup> Previous studies on the temperature dependence of the  $R$  for PUF-PAS also yielded inconsistent results. Increased  $R$  for some particle-bound PAHs was observed as temperature increases, which was explained with a shifting from particle to gas phase at higher temperatures.<sup>11,15</sup> However, a negative correlation was found for BDE-99, which is also likely to undergo gas–particle phase exchange.<sup>17</sup> Calibrations for selected pesticides conducted at different latitudes for XAD-PAS yielded higher  $R$  at higher temperatures.<sup>19</sup> However, this cannot be due to shifts in the atmospheric phase distribution because the gas–particle exchange behavior of these pesticides is not sensitive to temperature in the environmental temperature range. Here, we hypothesize that SVOCs distribute nonuniformly within the PSM and the PSM-side kinetic resistance could also affect  $R$ . This resistance might help explain the variation of  $R$  among chemicals and with temperatures. To explain the variation of  $R$  with sampling time, Chaemfa et al.<sup>8</sup> postulated a two-phase uptake processes: chemicals first sorb to the surface of PUF and then penetrate into the PUF at a slower rate. This is essentially similar to our PSM-side kinetic resistance hypothesis. However, no further investigation has sought to confirm this hypothesis that challenges the current PAS uptake theory.

In this study, we aim to (1) investigate whether PSM or housing differences cause the different sampling rate between XAD-PAS and PUF-PAS, (2) test our hypothesis on chemical distribution and kinetic resistance within PSM, and (3) quantify the effective diffusivity of chemical transfer within the PSM. To achieve these objectives, we performed a kinetic uptake experiment using concentrically segmented XAD and PUF positioned in the same type of sampler housing.

## MATERIALS AND METHODS

**Passive Sampling Media.** XAD packed in mesh cylinders and PUF were selected for this study because they are the most widely used passive sampling media (PSM) for SVOCs in air. Instead of the PUF disk commonly used in the “double-bowl” type PAS,<sup>2</sup> a cylindrical PUF plug (8 cm diameter, 8 cm high) was made from 1-cm-thick PUF sheets (Pacwill Environmental,

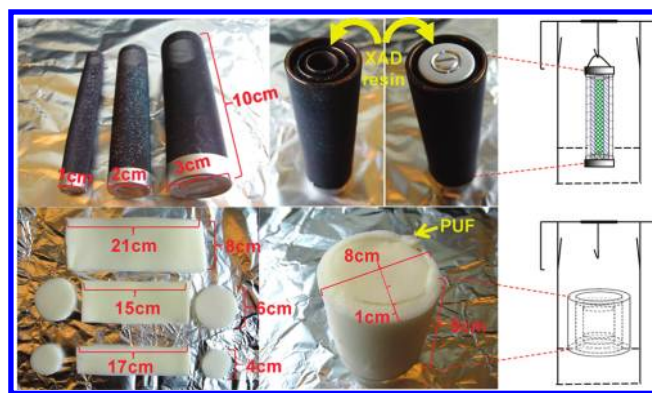


**Figure 1.** Design of the layered passive air sampling media (XAD and PUF) used to study the distribution of PCBs within the passive sampling medium.

density  $\sim 0.02$  g/cm<sup>3</sup>) and placed in the “cylindrical can” housing commonly used with XAD-PAS (Figure 1) to eliminate the influence of sampler housing design when comparing the uptake characteristics of the two PSM. The XAD-filled mesh cylinder and cylindrical PUF were concentrically segmented into three layers (outer, mid, and inner). The PSM layers can be separated upon sample retrieval. Detailed dimensions of the PSM are given in Figure 1. Before sampling, the segmented PUF components were sequentially cleaned with soap water and deionized water, and Soxhlet-extracted with acetone for 24 h and with petroleum ether for another 24 h. The XAD-2 resin was purchased and precleaned (Sigma-Aldrich).

**Chemicals.** Polychlorinated biphenyls (PCBs) were selected as the target chemicals for this study because the PCB congeners cover a wide range of partitioning properties (e.g., PSM/air partition coefficient), which also partially overlaps with other SVOCs of environmental interest such as organochlorine pesticides, polycyclic aromatic compounds, and brominated flame retardants. PSM (XAD and PUF)/air partition coefficients for individual PCB congeners, estimated using poly parameter linear free energy relationships<sup>13,18</sup> and recently updated PCB solute descriptors,<sup>19</sup> were compiled in Tables S1 and S2 in the Supporting Information (SI) and were used for further data analysis.

**Sampling Design.** Before deployment, the three layers of PSM were spiked with three different groups of deuration compounds (DCs) comprised of <sup>13</sup>C-labeled PCB congeners or nonlabeled PCB congeners that are not present in ambient air. Different groups of DCs were applied to different PSM layers. Detailed information on DCs and spiking procedure is provided in the SI. An unoccupied office previously identified as being contaminated with PCBs was selected as the sampling site. Duplicated XAD (PUF) samples were retrieved after been deployed for 0, 1 (0.5), 2 (1), 4 (2), 8 (4), 12 (8), and 24 (12) weeks. Deployment lengths for PUF-PAS were shorter, because we had anticipated faster uptake than for XAD-PAS. Upon retrieval, the layered PSMs were separated, individually sealed in precleaned aluminum foil and Ziploc bags, and stored at  $-20$  °C before extraction within 2 weeks. Along with the PAS, a low-volume active sampler (BGI Inc.,  $2.9 \pm 0.2$  m<sup>3</sup>/d) with a PUF-XAD-PUF sandwich (5 g of XAD between two 2-cm i.d.  $\times$  3-cm PUF plugs) as the sampling medium was used to measure the PCB air concentrations with monthly resolution. The sampling scheme is illustrated in Figure S1.

**Sample Extraction and Analysis.** Each sample was Soxhlet extracted for 24 h in  $\sim 500$  mL of petroleum ether (PUF) or 1:1

acetone/hexane (XAD and PUF-XAD-PUF sandwiches). The extract was rotoevaporated to  $\sim 2$  mL and eluted through a disposable pasteur pipet packed with dehydrated sodium sulfate to remove moisture. The eluent was blown down with high purity  $N_2$ , solvent exchanged to iso-octane, and reduced to  $\sim 0.5$  mL in a GC vial, to which 100 ng of mirex was added for volume correction and as internal standard for PCB quantification.

PCBs in the samples were analyzed with an Agilent 5890 gas chromatograph (GC) coupled with a JMS-800 double focusing high-resolution mass spectrometer (HRMS, resolution  $\geq 60,000$ ). The detailed method for instrumental analysis is described by Matsumura et al.<sup>20</sup> Briefly, 1.0  $\mu\text{L}$  of the sample was injected in splitless mode with the injector temperature at 280 °C. PCBs in the sample were separated using an HT8-PCB column (0.25 mm i.d.  $\times$  60 m, SGE Analytical Science) with helium (1 mL/min) as the carrier gas. The GC oven was programmed from 120 to 180 at 20 °C/min, to 260 at 2 °C/min, to 300 at 5 °C/min, and then held isothermal for 4 min. The HRMS was operated under EI and SIM mode with the interface and chamber operated at 260 °C.

**QA/QC.** All samples were duplicated to quantify reproducibility. Data analysis for all samples was based on both duplicates except for the XAD 12-month inner layer, of which one duplicate was lost during sample preparation. The relative difference between the passive sampling rates derived from duplicated samples was generally less than 10% (Figure S2). Duplicated field blanks for both XAD- and PUF-PAS were treated as time zero values in the analysis of chemical uptake kinetics. Prior to extraction, each sample was spiked with 100  $\mu\text{L}$  of 250 pg/ $\mu\text{L}$   $^{13}\text{C}_{12}$ -labeled PCB-77, -101, -141, and -178 (Cambridge Isotope) as surrogate standards. Recoveries of the four surrogate standards ranged between 74 and 131% with an interquartile range <15% (Figure S3).

**Derivation of Passive Air Sampling Rates.** Passive air sampling rates ( $R$ ,  $\text{m}^3/\text{d}$ ) and the PSM-side effective diffusivities ( $D_{E, \text{PSM}}$ ,  $\text{m}^2/\text{h}$ ) were obtained by linear least-squares fitting (LLSF) to all duplicated data points. For data below the LOD, random numbers between 0 and LOD were assigned.<sup>21,22</sup> The method of using LLSF to derive  $R$  has been applied in other studies.<sup>2,8</sup> Briefly,  $R$  equals the slope of the linear least-squares fitted line of the equivalent sampling volume ( $V_{\text{eq}}$ ) over the PAS deployment time;  $V_{\text{eq}}$  is calculated as the amount of a chemical sequestered in the PSM (sum of the three layers) divided by the ambient air concentration measured using the active air sampler.

**Derivation of the Effective Diffusivities on the PSM Side.** To derive  $D_E$  on the PSM side, a two-layered PSM mass balance model was developed (Figure S4, eqs S6–S14, and the relevant text in SI). The outer layer in the above-mentioned experiments is referred to as Layer 1; since few PCB congeners were detected in the inner layer, the inner and mid layers in the experiment were combined and are referred to as Layer 2 hereafter. Starting from the chemical mass balance equations (eqs S6 and S7) for the two layers, a relationship between the amounts of chemical sequestered in Layers 1 and 2 was derived

$$m_2(t) = \frac{1}{2} k_{\text{PSM12}} \frac{A_2}{V_1} [m_1(0) + m_1(t)]t + m_2(0) \quad (1)$$

where  $m_1(t)$  and  $m_2(t)$  [dimension: M] are the amount of the chemical sequestered in Layer 1 and 2 at time  $t$  [T];  $k_{\text{PSM12}}$  [ $\text{LT}^{-1}$ ] is the mass transfer coefficient for chemical diffusion between the two layers of the PSM, and  $k_{\text{PSM12}} = D_{E, \text{PSM}}/\delta$ , where  $D_{E, \text{PSM}}$  [ $\text{L}^2\text{T}^{-1}$ ] is the effective diffusivity of the chemical in the PSM and  $\delta$  [L] is the diffusion length;  $A_2$  [ $\text{L}^2$ ] is the area

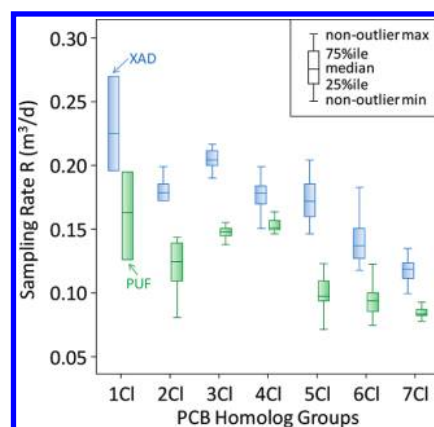


**Figure 2.** Comparison of the passive air sampling rates of PCB homologues between the passive sampling media of XAD and PUF positioned in the same type of cylindrical sampling housing.

between Layer 1 and 2;  $V_1$  [ $\text{L}^3$ ] is the Layer 1 volume of the PSM. Let  $X_t = [m_1(0) + m_1(t)] \cdot t$ ,  $Y_t = m_2(t)$ , and apply LLSF to  $X_t$  and  $Y_t$ , the slope of the fitted line equals to  $k_{\text{PSM12}} A_2 / (2V_1)$ , from which  $k_{\text{PSM12}}$  can be determined. Further, if  $\delta$  is known,  $D_{E, \text{PSM}}$  can be determined.

#### Mechanistic Model of Effective Diffusivity in Porous Media.

A previously developed modeling approach for the effective diffusivity of chemicals in porous media, such as soil and sediment, which considers sorption and tortuosity<sup>16,23</sup> was applied to fit the effective diffusivity in PUF ( $D_{E, \text{PUF}}$ ) derived in this study:

$$D_{E, \text{PUF}} = \Phi_A \cdot f \cdot D_A = \frac{1}{1 + r_{\text{SA}} \cdot K_{\text{PUF/A}}} \cdot f \cdot D_A \approx \frac{f}{r_{\text{SA}}} \cdot \frac{D_A}{K_{\text{PUF/A}}} \quad (2)$$

where  $D_{E, \text{PUF}}$  [ $\text{L}^2\text{T}^{-1}$ ] is the effective diffusivity in PUF,  $D_A$  [ $\text{L}^2\text{T}^{-1}$ ] is the molecular diffusivity in bulk air,  $\Phi_A$  [dimensionless] is the fraction of the chemical in the air-filled PUF pore space,  $f$  [dimensionless] is a correction factor related to intra-aggregate porosity and tortuosity,<sup>23</sup>  $r_{\text{SA}}$  [ $\text{L}^3(\text{PUF})\text{L}^{-3}(\text{A})$ ] is the volume ratio between the solid PUF material and the porous air space in PUF, and  $K_{\text{PUF/A}}$  [ $\text{L}^3(\text{A})\text{L}^{-3}(\text{PUF})$ ] is the chemical partition coefficient between PUF and air. The ratio  $f/r_{\text{SA}}$  is a property of the porous medium that decreases with increasing density and tortuosity of the PUF.

## RESULTS AND DISCUSSION

**Passive Air Sampling Rates.** To compare the performance of XAD and PUF, we studied the PCB uptake kinetics on the two PSM placed in housings of the same design (Figure 1). The median of the  $R$  for the PCB congeners in each homologue group ranged 0.12–0.23 and 0.08–0.16  $\text{m}^3/\text{d}$  for an XAD and PUF-based PAS, respectively (Figure 2).  $R$  values derived for the individual PCB congeners are reported in Table S3. Because the configurations of the PSM used in this study were different from those used previously, it is not feasible to directly compare  $R$  with those reported in other studies. Therefore,  $R$  ( $\text{m}^3/\text{d}$ ) was normalized to the PSM surface area ( $\text{dm}^2$ ) and the normalized sampling rate (SR,  $\text{m}^3/\text{d}/\text{dm}^2$ ) was used for comparison (Table S4). XAD-based SR ranged 0.11–0.32  $\text{m}^3/\text{d}/\text{dm}^2$ , which is approximately 5- to 10-fold lower than SR from previous outdoor calibrations for XAD-PAS.<sup>1,9,12</sup> This is in agreement with



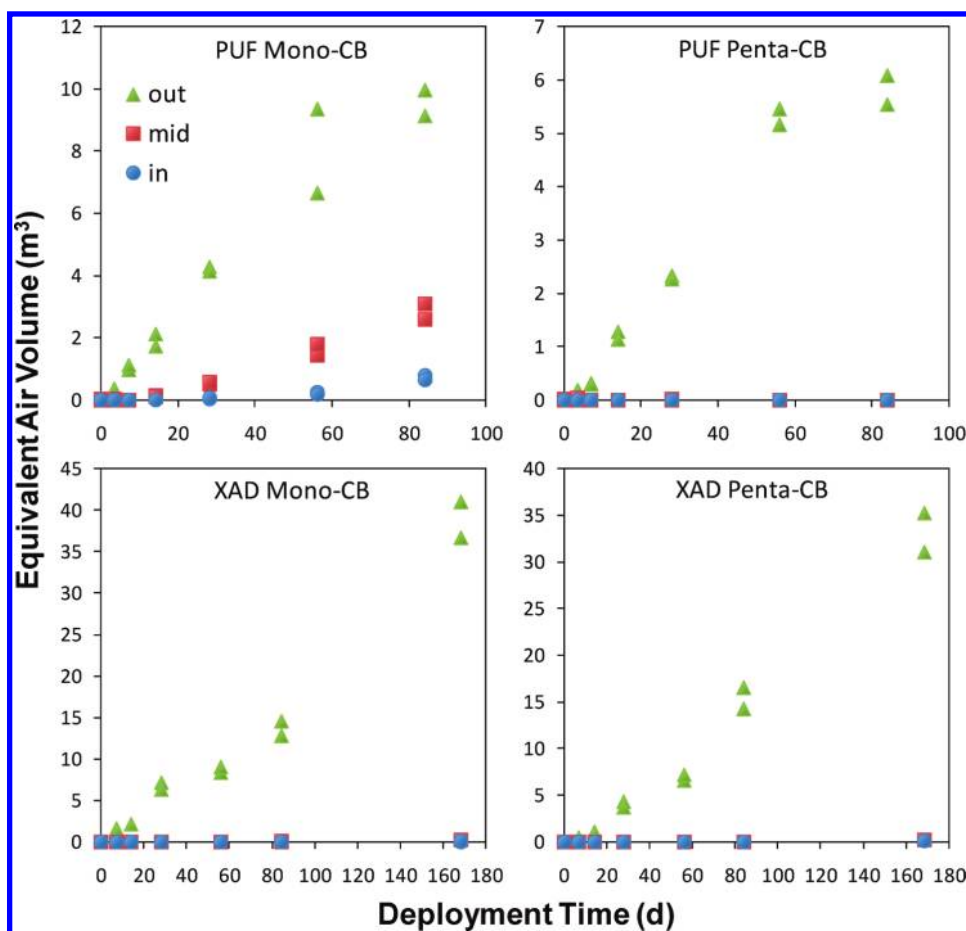


**Figure 3.** PCB accumulation and distribution in the outer, middle, and inner layers of the passive sampling media (PUF and XAD). Plots are based on duplicated measurements. Mono-PCB (PCB-1) and Penta-PCB (PCB-98/95) are used to illustrate the differences between PCBs of different chlorination or physicochemical properties.

previous studies on the PUF-PAS, which indicate that outdoor SR can be as much as  $\sim 50$ -fold higher than indoor SR.<sup>10,11</sup> The lower SR observed indoors by this and other studies can be attributed to the different extent of air movement indoors and outdoors. Relatively wind-still indoor conditions tend to increase the thickness of the air boundary layer surrounding the PSM and reduce  $R$ . The low air movement indoors could also increase the resistance to chemical transfer from ambient air into the PAS housing, which could possibly cause a “starvation” effect<sup>24</sup> and make the air concentration within the housing lower than the ambient air. However, such an effect would exist and lower the passive sampling rate only if the resistance for a chemical to diffuse into the housing from ambient air is higher than that for chemical uptake by the PSM. Because it is difficult to measure the actual air concentration of SVOC within the PAS housing without disturbing its normal operational conditions, such a “starvation” effect on PAS for SVOC has so far not been confirmed experimentally.

PUF-based SRs of this study ranged  $0.02\text{--}0.07\text{ m}^3/\text{d}/\text{dm}^2$ , which is  $\sim 5$ - and  $\sim 30$ -fold lower than the calibrated indoor SR by Hazrati and Harrad<sup>10</sup> and Shoeib and Harner.<sup>2</sup> Apart from interstudy variations ( $\sim 5$  times difference for the same type of PAS between refs 2 and 10), different sampler configurations could provide a possible explanation for the lower PUF-based SR observed here. In this study, a PUF-cylinder was positioned in a “cylindrical can” rather than the more commonly used arrangement of a disk in a “double bowl” housing.<sup>2,8,10,11</sup> This different

configuration could increase the thickness of stagnant air around the PUF, increase the kinetic resistance for a chemical to diffuse into the housing from ambient air, and thus lower the SR. Evidence of the effect of sampler configuration on passive sampling rates can also be found in studies by Tao et al.<sup>25,26</sup> PUF disks positioned in a more confined housing had  $\sim 10$ -fold lower SR than PUF disks in a “double bowl” shelter. Such evidence of the effect of sampler configuration on passive sampling rate indicates that the housing design may also contribute to the kinetic resistance to chemical uptake.

The homologue-specific  $R$  decreases from the lighter to the heavier PCBs for both PSMs (Figure 2). This is in contrast with previous studies on the PUF-PAS, which found higher  $R$  for heavier congeners.<sup>8,10,11</sup> A higher fraction of heavier congeners is particle-bound in air. The higher  $R$  for heavier congeners was attributed to particles being captured by the PUF-disk.<sup>8,10,11</sup> Unlike the PUF-PAS, in which particle-bound chemicals were often detected,<sup>27,28</sup> the XAD-PAS is unlikely to trap atmospheric particles since few particle-bound chemicals have ever been detected in XAD-filled mesh cylinders positioned in a cylindrical housing.<sup>5</sup> The semienclosed configuration of the “cylindrical can” shelter greatly limits advective air flow into the housing and thus few particles may enter the housing and get trapped on the PSM. Excluding the effect of particle-bound chemicals, chemical sequestration on the PSM is mainly determined by chemical transport from the ambient air to the PSM via diffusion in the gas

phase. This is supported by the positive correlations between the homologue-specific passive sampling rate and the gaseous molecular diffusivity of the chemicals (Figure S5).

**Evidence of Kinetic Resistance on Chemical Transfer within PSM.** The kinetics of PSM-side mass transfer of the DCs and PCBs from air was investigated by analyzing the amount sequestered in each layer after different deployment times.

**PCB Uptake from Air.** Higher PCB levels were found in the outer layer than in the middle and inner layer over the whole sampling period (Figure 3 and Tables S5 and S6). Within the first month of PAS deployment, the PCBs were either not detected in the middle or inner layers of PUF or detected at levels no different from the blanks. Mono-CBs could be detected in the middle and inner PUF layer after 4 and 8 weeks of deployment, respectively. Nevertheless, even after 12 weeks of deployment, the amount of mono-CBs in the middle and inner PUF layers was only ~20% and ~5% of that in the outer layer (Figure 3). Heavier PCBs could hardly be detected in the inner PUF layer, even after 12 weeks. For the mono- to tetra-PCBs detected in the middle PUF layer, the ratio of the amount in middle and outer layer was generally lower for the heavier congeners. No detectable amounts of penta-CBs and higher chlorinated PCBs could be found penetrating to the middle layer even after 12 weeks (Figure 3). Lighter PCBs appeared to diffuse more easily to the inner PUF layer: mono-CBs could diffuse through the 2-cm outer and middle PUF layer into the inner layer. This is because lighter PCBs have lower sorption affinity to PUF (i.e., a lower  $K_{\text{PUF/A}}$ ), allowing for a higher fraction to be in the gas phase of the PUF pores. The nonuniform PCB distribution within the PSM contradicts the assumption in the current passive air sampling theory<sup>7</sup> describing chemical uptake in PAS.<sup>2,3</sup>

Compared to the PUF, less of the mono-CBs were found penetrating into the XAD (Figure 3). Even after 24 weeks, the amount sequestered in the middle layer was only ~1% of that in the outer layer and no PCBs could be detected in the inner layer. This is in line with  $K_{\text{XAD/A}}$  being higher than  $K_{\text{PUF/A}}$  for individual PCB congeners (Tables S1 and S2), which make them less likely to be in the porous air phase and available for diffusion through the XAD-PSM. However, despite different  $K_{\text{XAD/A}}$  values, the amount of PCBs sequestered in the middle layer relative to that in the outer layer was very similar for different PCB homologues; even for the heavier PCB homologues such as hepta-CBs the middle layer contained approximately ~1% of the amount in the outer layer. We attribute this to the incomplete shielding of the middle XAD layer from ambient air. The XAD resin may have settled during the deployment period and left the upper part of the XAD in the inner mesh cylinders partially exposed to ambient air. Therefore, we can only infer that less than 1% of the PCBs in the outer XAD layer would penetrate to the middle layer by diffusion through the pores. This low diffusion rate also indicates that even if only 1% of the middle XAD layer was exposed to ambient air, the amount detected in the middle layer can not reflect the diffusion across the outer layer. Therefore, we do not further interpret the data for the layered XAD-PSM but focus on the layered PUF-PSM, of which the inside layer was completely covered by the outer one.

**Depuration Compounds.** Transport of the spiked DCs between the PSM layers was observed. The data for the DCs are presented (Figures S6 and S7) and discussed in the SI.

**Mass Transfer Coefficient for Chemical Diffusion between the Two PUF Layers ( $k_{\text{PUF12}}$ ).**  $k_{\text{PUF12}}$  was derived by fitting the amount of chemical accumulated in each PUF layer to the

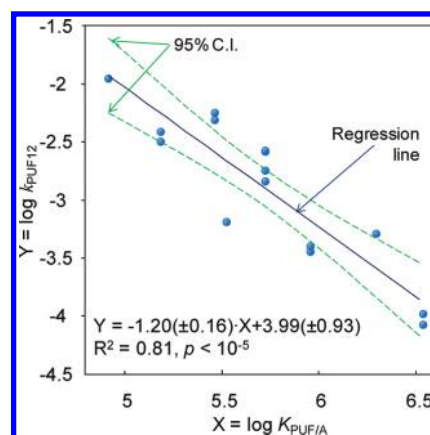


**Figure 4.** Relationship between the PUF–air partition coefficients ( $K_{\text{PUF/A}}$  at 20 °C) and the mass transfer coefficients for chemical diffusion between the two PUF layers ( $k_{\text{PUF12}}$ , m/h). The data points represent selected mono-, di-, and tri-CB congeners that penetrated into the inner PUF with detectable amounts. The dashed lines indicate 95% confidence interval of the regression model.

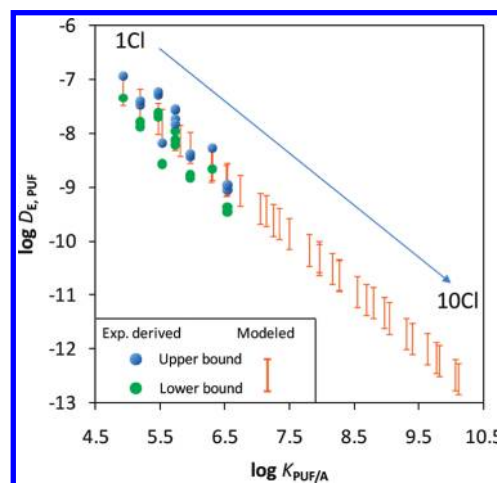


**Figure 5.** Relationship between the effective diffusivity in PUF ( $D_{\text{E,PUF}}$ ,  $\text{m}^2/\text{h}$ ) and the PUF/air partition coefficient ( $K_{\text{PUF/A}}$ ) for PCBs. The upper- and lower-bound experimentally derived  $D_{\text{E,PUF}}$  values were based on a diffusion length of 1 and 2.5 cm, respectively. The upper- and lower-bound modeled  $D_{\text{E,PUF}}$  values were based on a  $f/r_{\text{SA}}$  value of 0.14 and 0.53, respectively.

two-layered mass balance model (eq 1).  $k_{\text{PUF12}}$  was calculated only if the coefficient of determination of the LLSF was over 0.7. The  $k_{\text{PUF12}}$  could only be derived for mono-, di-, and tri-CBs because heavier PCBs could not be detected in Layer 2. The derived  $k_{\text{PUF12}}$  ranged from  $4.0 \times 10^{-4}$  m/h for PCB-28 (tri-CB) to  $1.1 \times 10^{-2}$  m/h for PCB-1 (mono-CB) (Figure 4). A negative correlation (Spearman's  $\rho = 0.91$ ,  $p < 10^{-4}$ ) was found between  $k_{\text{PUF12}}$  and the PUF–air partition coefficients ( $K_{\text{PUF/A}}$ ). A simple regression model to predict  $k_{\text{PUF12}}$  from  $K_{\text{PUF/A}}$  (Figure 4) shows that 81% of the variation in the experimentally derived  $k_{\text{PUF12}}$  can be accounted for by the variation in  $K_{\text{PUF/A}}$ . The  $k_{\text{PUF12}}$  is related to the diffusion distance within the PUF and thus affected by the dimensions of the PUF. To exclude this factor, we derived the effective diffusivity ( $D_{\text{E,PUF}}$ ).

**Effective PSM-Side Diffusivities ( $D_{\text{E,PUF}}$ ).** As the product of  $k_{\text{PUF12}}$  and diffusion length,  $D_{\text{E,PUF}}$  excludes the effect of PUF

dimensions and should only depend on the properties of the PUF and chemical. Because  $k_{\text{PUF}12}$  was derived from chemical concentrations in two discrete PUF layers of finite thickness, we do not have information on the diffusion length within the PUF. Therefore, a range between 1 cm (thickness of Layer 1) and 2.5 cm (thickness of Layer 1 plus half the thickness of Layer 2) was used to represent the potential distance that chemicals diffusing from Layer 1 to Layer 2 are traversing.

The magnitude of  $D_{\text{E,PUF}}$  ranged from  $10^{-9}$  m<sup>2</sup>/h for tri-CBs to  $10^{-7}$  m<sup>2</sup>/h for mono-CBs (Figure 5). Although chemical diffusion in PUF occurs in the air-filled pore space, the effective diffusivity in PUF is lower than the diffusivity in air by a factor of  $10^5$ – $10^7$ . The low diffusivity in PUF is mainly attributed to the relatively large  $K_{\text{PUF/A}}$  and thus a low fraction of the chemical in the porous air phase, where chemical diffusion within PUF occurs. Another factor lowering the chemical diffusivity in PUF is the tortuous diffusion pathway within the PUF, which increases the diffusion length and decreases  $D_{\text{E,PUF}}$ . The influence of these factors on  $D_{\text{E,PUF}}$  is also illustrated by the mechanistic model of chemical diffusion in porous media (eq 2). Fitting the  $D_{\text{E,PUF}}$  (upper- and lower-bound value) derived in this study, we estimated  $f/r_{\text{SA}}$  ranges between 0.18 (95% CI: 0.14–0.21) and 0.45 (95% CI: 0.35–0.53). Based on the model,  $D_{\text{E,PUF}}$  values were calculated for all PCB congeners (Figure 5).  $D_{\text{E,PUF}}$  decreases by over 5 orders of magnitude from mono- to deca-CB. This variation in  $D_{\text{E,PUF}}$  is mainly due to the variation in  $K_{\text{PUF/A}}$ , because  $D_{\text{A}}$  varies by less than 50% among different PCB congeners (Figure S8). The upper- and lower-bound  $D_{\text{E,PUF}}$  from the model differ by  $\sim 0.6$  log-unit, which represents the range of  $f/r_{\text{SA}}$  caused by potential variations of physical PUF properties. Using PUF with densities of 0.021 and 0.035 g/cm<sup>3</sup>, Chaemfa et al.<sup>29</sup> found no significant difference in sampling rates during 12 weeks of uptake. Based on our hypothesis, slightly higher uptake rates would be expected in low density PUF. This finding suggests that in the currently used PUF,  $f/r_{\text{SA}}$  varies less than the difference between our upper- and lower-bound values. Interestingly, although overall uptake rates were not significantly different, Chaemfa et al. noted a faster uptake of some PCBs in the low-density PUF during early uptake.<sup>29</sup>

**Further Comments on the PSM-Side Kinetic Resistance and Its Implications.** Based on our experimental results and evidence from previous studies,<sup>8,9,29</sup> we conclude that a kinetic resistance to chemical transfer exists within the PSM (PUF and XAD).

The PSM in this study was a cylindrical PUF plug of 8-cm diameter. However, because  $D_{\text{E,PUF}}$  of a chemical only depends on the properties of the PUF material but not on its shape, it should be possible to extrapolate the results of this study to the widely used 1-cm PUF disk. Because the experiment was conducted indoors and the PSM were positioned in a housing that effectively shields the wind, advective transport of chemicals within the PSM likely did not occur. This agrees with Bohlin et al.,<sup>28</sup> who observed only a minor influence of wind on PUF-PAS deployed indoors. In PAS campaigns conducted outdoors, however, wind is likely to pass through the “double bowl”-type housing, resulting in increasing sampling rates with increasing wind speed.<sup>30</sup> Such a wind effect on the sampling rate can be caused by a decrease in the thickness of the air boundary layer and/or an increased effective diffusivity within the PSM. According to CFD simulations on the PUF-PAS,<sup>31</sup> the wind velocity approaches zero at the PUF surface. Therefore, if the wind does not blow directly toward the PUF, wind should have little, if any, effect on  $D_{\text{E,PUF}}$ . However, the CFD simulations rely on assumed

scenarios of wind and other conditions. Based on the existing information on PAS under environmental conditions outdoors, we cannot exclude the possibility of advective chemical transport within the PSM. Further studies are needed to understand the potential advective transport within PSM and its effect on the PSM-side kinetic resistance under various wind conditions.

The nonuniform chemical distribution within the PSM affects the calculation of the maximum linear uptake capacity of a PAS and the characteristic times of linear uptake or equilibration. Assuming a uniform chemical distribution within the PSM<sup>3</sup> will lead to an overestimation of both the uptake capacity and the characteristic times because only the outer layer of the PSM is available for the sampled chemicals. Knowledge of the nonuniform chemical distribution can also help optimization of PAS design. Thinner PSM with a high surface area increase the sampling rate  $R$  without a significant loss in uptake capacity.

The nonuniform chemical distribution within PSM also challenges the current passive air sampling theory.<sup>3</sup> Based on the two-film model,<sup>7</sup> it assumes the sampled chemical is uniformly distributed within the PSM and a kinetic resistance to chemical uptake and loss only arises from the air boundary layer. This conceptual approach failed to explain chemical- and temperature-specific passive sampling rates,<sup>9,11</sup> because the experimentally observed variation of  $R$  between chemicals and with temperatures was much larger than that can be explained by the compound-specificity and temperature dependence of  $D_{\text{A}}$ .<sup>1,9</sup> In this study, we found that the PSM-side kinetic resistance correlates with  $K_{\text{PUF/A}}$ , which varies more among different chemicals and at different temperatures than  $D_{\text{A}}$ . Qualitatively, this agrees with the experimental observations. It would be desirable to quantitatively compare the kinetic resistance (i.e., reciprocal of the mass transfer coefficients) introduced by air boundary layer and PSM. However, we currently do not know the thickness of the boundary layer or the average diffusion length within the PSM, which are necessary to convert the diffusivities to mass transfer coefficients. Because  $D_{\text{E,PUF}}$  are more than 7 orders of magnitude lower than  $D_{\text{A}}$ , the PSM side resistance will play a role in the overall uptake as long as the average diffusion length within the PSM exceeds  $1/10^7$  of the boundary layer thickness. A model that does not rely on the assumption of a uniform chemical distribution within the PSM will be required to quantitatively understand the PSM-side kinetic resistance and its influence on sampling rates.

The current passive air sampling theory has also been used to describe the loss of DCs from the PSM and to derive sampler-specific sampling rates.<sup>3,30</sup> This approach relies on the assumption that the uptake of the sampled chemicals and the loss of the DCs are subjected to the same kinetic resistances.<sup>30</sup> This assumption would likely be true if the kinetic resistance of the air boundary layer were rate-limiting. However, because the kinetic resistance on the PSM side is not negligible, the kinetic resistance to uptake and loss would only be identical if the distribution of DCs and sampled chemicals within the PSM were the same. Such rigid conditions are impossible to meet because the distribution of the sampled chemicals within the PSM is unknown beforehand. Therefore, such uncertainty should be considered when interpreting PAS-based air concentrations calculated using  $R$  derived from the loss of DCs. Further efforts are necessary to quantify and correct the uncertainty of  $R$  derived from the loss of DCs.

## ■ ASSOCIATED CONTENT

**S Supporting Information.** Further information on experimental methods,  $Q_{\text{A/QC}}$ , model derivation,  $K_{\text{XAD/Air}}$  and  $K_{\text{PUF/Air}}$



for PCBs, congener-specific  $R$ , and further interpretation on the results. This material is available free of charge via the Internet at <http://pubs.acs.org>.

## AUTHOR INFORMATION

### Corresponding Author

\*Phone: 416-287-7225; e-mail: [frank.wania@utoronto.ca](mailto:frank.wania@utoronto.ca).

## ACKNOWLEDGMENT

We are grateful to James Armitage for sharing the idea for the design of the described experiments and to the Canadian Foundation for Climate and Atmospheric Sciences and the Natural Sciences and Engineering Research Council of Canada for funding. X.Z. acknowledges the Centre for Global Change Science at the University of Toronto for supporting the visit to HIES.

## REFERENCES

- Wania, F.; Shen, L.; Lei, Y. D.; Teixeira, C.; Muir, D. C. G. Development and calibration of a resin-based passive sampling system for monitoring persistent organic pollutants in the atmosphere. *Environ. Sci. Technol.* **2003**, *37*, 1352–1359.
- Shoeb, M.; Harner, T. Characterization and comparison of three passive air samplers for persistent organic pollutants. *Environ. Sci. Technol.* **2002**, *36*, 4142–4151.
- Bartkow, M. E.; Booi, K.; Kennedy, K. E.; Müller, J. F.; Hawker, D. W. Passive air sampling theory for semivolatile organic compounds. *Chemosphere* **2005**, *60*, 170–176.
- Zhang, X. M.; Diamond, M. L.; Robson, M.; Harrad, S. Sources, emissions, and fate of polybrominated diphenyl ethers and polychlorinated biphenyls indoors in Toronto, Canada. *Environ. Sci. Technol.* **2011**, *45*, 3268–3274.
- Shunthirasingham, C.; Oyiliagu, C. E.; Cao, X. S.; Gouin, T.; Wania, F.; Lee, S. C.; Pozo, K.; Harner, T.; Muir, D. C. G. Spatial and temporal pattern of pesticides in the global atmosphere. *J. Environ. Monit.* **2010**, *12*, 1650–1657.
- Bohlin, P.; Jones, K. C.; Levin, J. O.; Lindahl, R.; Strandberg, B. Field evaluation of a passive personal air sampler for screening of PAH exposure in workplaces. *J. Environ. Monit.* **2010**, *12*, 1437–1444.
- Lewis, W. K.; Whitman, W. G. Principles of gas absorption. *Ind. Eng. Chem.* **1924**, *16*, 1215–1220.
- Chaemfa, C.; Barber, J. L.; Gocht, T.; Harner, T.; Holoubek, I.; Klanova, J.; Jones, K. C. Field calibration of polyurethane foam (PUF) disk passive air samplers for PCBs and OC pesticides. *Environ. Pollut.* **2008**, *156*, 1290–1297.
- Gouin, T.; Wania, F.; Ruepert, C.; Castillo, L. E. Field testing passive air samplers for current use pesticides in a tropical environment. *Environ. Sci. Technol.* **2008**, *42*, 6625–6630.
- Hazrati, S.; Harrad, S. Calibration of polyurethane foam (PUF) disk passive air samplers for quantitative measurement of polychlorinated biphenyls (PCBs) and polybrominated diphenyl ethers (PBDEs): Factors influencing sampling rates. *Chemosphere* **2007**, *67*, 448–455.
- Melymuk, L.; Robson, M.; Helm, P. A.; Diamond, M. L. Evaluation of passive air sampler calibrations: Selection of sampling rates and implications for the measurement of persistent organic pollutants in air. *Atmos. Environ.* **2011**, *45*, 1867–1875.
- Hayward, S. J. Fate of current-use pesticides in the Canadian atmosphere. Ph.D. Thesis. University of Toronto, Toronto, 2010.
- Hayward, S. J.; Lei, Y. D.; Wania, F. Sorption of a diverse set of organic chemical vapors onto XAD-2 resin: Measurement, prediction and implications for air sampling. *Atmos. Environ.* **2011**, *45*, 296–302.
- Hayward, S. J.; Gouin, T.; Wania, F. Comparison of four active and passive sampling techniques for pesticides in air. *Environ. Sci. Technol.* **2010**, *44*, 3410–3416.
- Klanova, J.; Eupr, P.; Kohoutek, J.; Harner, T. Assessing the influence of meteorological parameters on the performance of polyurethane foam-based passive air samplers. *Environ. Sci. Technol.* **2008**, *42*, 550–555.
- Schwarzenbach, R. P.; Gschwend, P. M.; Imboden, D. M. *Environmental Organic Chemistry*, 2nd ed.; Wiley: Hoboken, NJ, 2003.
- Chaemfa, C.; Barber, J. L.; Moeckel, C.; Gocht, T.; Harner, T.; Holoubek, I.; Klanova, J.; Jones, K. C. Field calibration of polyurethane foam disk passive air samplers for PBDEs. *J. Environ. Monit.* **2009**, *11*, 1859–1865.
- Kamprad, I.; Goss, K. U. Systematic investigation of the sorption properties of polyurethane foams for organic vapors. *Anal. Chem.* **2007**, *79*, 4222–4227.
- van Noort, P. C. M.; Haftka, J. J. H.; Parsons, J. R. Updated Abraham solvation parameters for polychlorinated biphenyls. *Environ. Sci. Technol.* **2010**, *44*, 7037–7042.
- Matsumura, C.; Tsurukawa, M.; Nakano, T.; Ezaki, T.; Ohashi, M. Elution orders of all 209 PCBs congeners on capillary column HT-8-PCB. *J. Environ. Chem.* **2002**, *12*, 855–866.
- Antweiler, R. C.; Taylor, H. E. Evaluation of statistical treatments of left-censored environmental data using coincident uncensored data sets: I. Summary statistics. *Environ. Sci. Technol.* **2008**, *42*, 3732–3738.
- Aruga, R. Treatment of responses below the detection limit: some current techniques compared by factor analysis on environmental data. *Anal. Chim. Acta* **1997**, *354*, 255–262.
- Wu, S. C.; Gschwend, P. M. Sorption kinetics of hydrophobic organic-compounds to natural sediments and soils. *Environ. Sci. Technol.* **1986**, *20*, 717–725.
- Brown, R. H. The use of diffusive samplers for monitoring of ambient air. *Pure Appl. Chem.* **1993**, *65*, 1859–1874.
- Tao, S.; Cao, J.; Wang, W. T.; Zhao, J. Y.; Wang, W.; Wang, Z. H.; Cao, H. Y.; Xing, B. S. A passive sampler with improved performance for collecting gaseous and particulate phase polycyclic aromatic hydrocarbons in air. *Environ. Sci. Technol.* **2009**, *43*, 4124–4129.
- Tao, S.; Liu, Y. N.; Xu, W.; Lang, C.; Liu, S. Z.; Dou, H.; Liu, W. X. Calibration of a passive sampler for both gaseous and particulate phase polycyclic aromatic hydrocarbons. *Environ. Sci. Technol.* **2007**, *41*, 568–573.
- Chaemfa, C.; Wild, E.; Davison, B.; Barber, J. L.; Jones, K. C. A study of aerosol entrapment and the influence of wind speed, chamber design and foam density on polyurethane foam passive air samplers used for persistent organic pollutants. *J. Environ. Monit.* **2009**, *11*, 1135–1139.
- Bohlin, P.; Jones, K. C.; Strandberg, B. Field evaluation of polyurethane foam passive air samplers to assess airborne PAHs in occupational environments. *Environ. Sci. Technol.* **2010**, *44*, 749–754.
- Chaemfa, C.; Barber, J. L.; Kim, K. S.; Harner, T.; Jones, K. C. Further studies on the uptake of persistent organic pollutants (POPs) by polyurethane foam disk passive air samplers. *Atmos. Environ.* **2009**, *43*, 3843–3849.
- Moeckel, C.; Harner, T.; Nizzetto, L.; Strandberg, B.; Lindroth, A.; Jones, K. C. Use of depuration compounds in passive air samplers: Results from active sampling-supported field deployment, potential uses, and recommendations. *Environ. Sci. Technol.* **2009**, *43*, 3227–3232.
- Thomas, J.; Holsen, T. M.; Dhaniyala, S. Computational fluid dynamic modeling of two passive samplers. *Environ. Pollut.* **2006**, *144*, 384–392.